Investigation of New Ionic Plastic Crystals in Tetraalkylammonium Tetrabuthylborate

Tomoyuki Hayasaki[a], Satoru Hirakawa[b], and Hisashi Honda[a,b]

[a] Graduate School of Nanobioscience, Yokohama City University, Kanazawa-ku, Yokohama, 236-0027, Japan

[b] International College of Arts and Sciences, Yokohama City University, Kanazawa-ku, Yokohama, 236-0027, Japan

Reprint requests to H. H.; E-mail: hhonda@yokohama-cu.ac.jp

Z. Naturforsch. **69a**, 433 – 440 (2014) / DOI: 10.5560/ZNA.2014-0029
Received December 24, 2013 / revised March 31, 2014 / published online June 18, 2014

New plastic crystals of NEt_3PrBBu_4 and $NEt_2Pr_2BBu_4$ were formed in a new region of ionic plastic crystal. In this area, globular cations and anions are assembled by weak interactions. Differential scanning calorimeter (DSC) measurements of these salts showed a low entropy change of 19.6 and 14.0 $J\,K^{-1}\,mol^{-1}$ at each melting point, respectively. On the basis of solid-state ^1H and ^{13}C nuclear magnetic resonance (NMR) spectra and electrical conductivity measurements, isotropic reorientation and ion transfer of globular cations and anions were detected in these crystals. The other compounds of $NEt_xMe_{(4-x)}BBu_4$ ($x = 1-3$) showed tumbling motions and low activation energies of self-diffusion in crystals.

Key words: Plastic Crystal; Ionic Conductor; ^1H MAS NMR; ^{13}C MAS NMR.

1. Introduction

Plastic crystals are soft materials in solids. Since the constituents are isotropically rotated at each crystal-lattice point, small entropy changes at each melting point ($\Delta S_{mp} < 20\,J\,K^{-1}\,mol^{-1}$) and a large ΔS value at a transition temperature between solid phases can be detected [1]. In addition, self-diffusion of constituent particles is observed in plastic phases. This translation causes plasticity in solid substances. A plastic crystal can be classified as either ionic or molecular based upon its constituent particles. In molecular plastic crystals, globular molecules, e. g. fullerene, adamantane, tetrachloromethane, etc., have plastic phases [2 – 9]. The globular molecular shapes and weak intermolecular attractions are key points for isotropic reorientation and self-diffusion of molecules with low activation energies. In contrast, ordinal ionic plastic crystals are formed by a globular ion and a non-globular counter ion with formulas MNO_2 (M = K, Rb, Cs, Tl, and NH_4) [10 – 24], $[C_5H_{10}N(CH_3)_2]SCN$ [25], $N(CH_3)_4N_3$ [26], piperidinium X (X = ClO_4, PF_6, NO_3) [27, 28], etc. Based on nuclear magnetic resonance (NMR) studies of MNO_2, a revolving door model has been proposed for ionic translation [23, 29]. In this model, isotropic reorientation rates of the plane anion (the revolving gate) are slow enough for the cation (the human) to diffuse through the plane formed by the anions. From the translating cation's point of view, the anions appear frozen. That is, the translation model is the difference between molecular and ionic plastic crystals. The difference is caused by constituents' shapes and strengths of interactions acting on particles. Based on this fact, we have proposed a new type of ionic plastic crystal in which a globular cation and anion perform isotropic reorientation if the Coulomb force among the ions is weak enough [30]. In the new region of plastic crystal, we have succeeded in showing the new type of ionic plastic crystals as reported for NR_4BEt_3Me (R = Me, Et) and $NEt_xR'_{(4-x)}BEt_3Me$ (R′ = Me, Pr. $x = 1-3$) [30]. In contrast, NR_4BBu_4 (R = Me, Et, Pr, Bu, Pen) salts have no plastic phases [31]. In this study, we treated $NEt_xR_{(4-x)}BBu_4$ (R = Me, Pr. $x = 1-3$) crystals, in order to investigate ionic plastic crystals and reveal ionic dynamics in the crystals.

Table 1. Entropy changes (ΔS) in J mol^{-1} K^{-1} at phase transition temperature and melting point and activation energies (E_a) of ion transfer in kJ mol^{-1} observed in $NEt_xR_{(4-x)}BBu_4$ ($x = 1-3$, R = Me, Pr) salts. Each transition temperature is displayed in parenthesis (unit is K).

	ΔS_{tr2} (T_{tr2})	ΔS_{tr1} (T_{tr1})	ΔS_{mp} (T_{mp})	E_a
$NEtMe_3BBu_4$	28.2 (332.7)	8.7 (371.2)	28.5 (388.1)	$50 \pm 10^*$
$NEt_2Me_2BBu_4$		14.3 (340.9)	24.7 (382.4)	$70 \pm 10^*$
NEt_3MeBBu_4	38.0 (265.0)	18.0 (306.0)	25.3 (382.0)	60 ± 20
NEt_3PrBBu_4		47.0 (286.3)	19.6 (343.4)	60 ± 10
$NEt_2Pr_2BBu_4$		49.5 (267.2)	14.0 (307.9)	65 ± 20
$NEtPr_3BBu_4$	5.5 (254.0)	8.9 (268.0)	44.1 (295.2)	–**

* E_a values in the highest solid phase. ** E_a values could not be obtained because of low T_{mp}.

2. Experiment

Crystals of $NEt_xR_{(4-x)}BBu_4$ (R = Me, Pr. $x = 1-3$) were prepared by adding $LiBBu_4$ into $NEt_xR_{(4-x)}Br$ in aqueous solution. For preparation of $LiBBu_4$, the previously reported recipe [32] was slightly altered. The crude samples were recrystallized from a mixed solution of acetone and water.

Differential scanning calorimeter (DSC) spectra were obtained with a Shimadzu DSC-60 and Seiko Instruments Inc. SSC/5200 calorimeter with a reference sample of Al_2O_3. The samples were heated from ca. 210 K at rates of 5 K min^{-1}. Electrical conductivity measurements were performed at 1 kHz with a two-terminal method employing an Andou AG-4303 LCR meter equipped with an aluminium sheet. The powdered sample was pressed into a disc of 1 cm in diameter and ca. 1 mm thickness. For measurements, the air around the probe was replaced by dry N_2 gas. Solid-state ^{1}H NMR spectra were recorded at a Larmor frequency of 600.13 MHz using a Bruker Avance 600 spectrometer (14.01 T). The samples were packed in a ZrO_2 rotor with an outer diameter of 4.0 mm. A magic-angle-spinning (MAS) method with 10 kHz was used. Solid-state ^{13}C NMR spectra were observed at a Larmor frequency of 150.92 MHz using the same spectrometer. The same sample tubes as those of the ^{1}H measurements were employed. ^{13}C NMR spectra were obtained with a ^{1}H decoupling pulse sequence. A cross-polarization (CP) method was also employed to detect motional modulation in the Hartmann–Hahn condition.

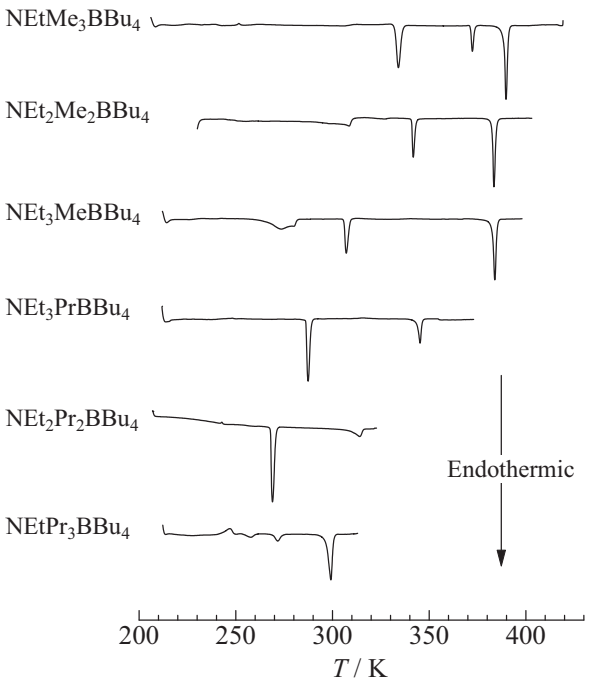

Fig. 1. DSC thermograms of $NEt_xR_{(4-x)}BBu_4$ ($x = 1-3$, R = Me, Pr).

Density functional theory (DFT) simulation was performed to assign NMR peaks and to estimate line-widths observed on ^{1}H and ^{13}C NMR spectra. As it has been demonstrated in the previous report [30] that a B3LYP/6-311+G** function in the Gaussian 03 computer program [33] can explain the ^{13}C NMR chemical shift (CS) values and line-widths observed in alkylammonium ions and a BEt_3Me^- ion well, the same procedure was used in this study.

3. Results and Discussion

3.1. Results of DSC and Electrical Conductivity

DSC thermograms observed in $NEt_xR_{(4-x)}BBu_4$ (R = Me, Pr. $x = 1-3$) crystals are shown in Figure 1. The variation appearing at the initial temperature range

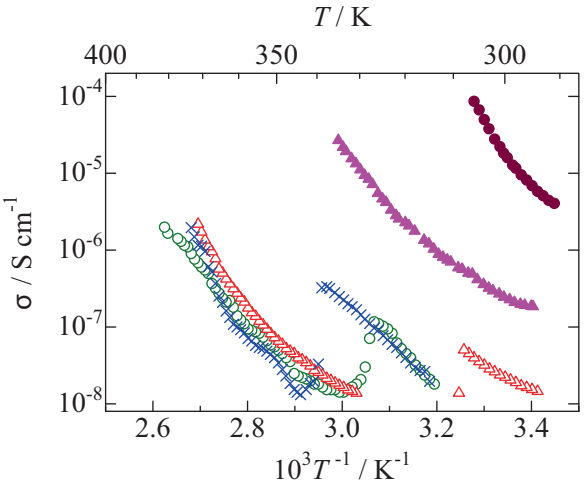

Fig. 2 (colour online). Electrical conductivity of $NEtMe_3BBu_4$(○), $NEt_2Me_2BBu_4$(×), $NEtMe_3BBu_4$(△), NEt_3PrBBu_4(▲), $NEt_2Pr_2BBu_4$(●) as a function of temperature.

(whole measurements were started at the low temperature) is due to instrument noise. In this paper, the symbols T_{mp} and T_{tr1}, T_{tr2}, etc., are employed to indicate the phase-transition temperatures at the melting point and in solid phases moving from higher to lower temperatures; and Phase I, Phase II, etc., are used to designate the solid phases from the highest-temperature solid-phase of each crystal. Entropy changes at the melting point (ΔS_{mp}) and at each transition temperature (ΔS_{tr1} and ΔS_{tr2}) obtained in each crystal are listed in Table 1. Small ΔS_{mp} values satisfying the condition of plastic crystal ($< 20\,J\,K^{-1}\,mol^{-1}$ [1]) were obtained in NEt_3PrBBu_4 and $NEt_2Pr_2BBu_4$. In addition, large entropy changes in solid phases were recorded in these two compounds. In the case of $NEt_2Me_2BBu_4$ and NEt_3MeBBu_4, small ΔS_{mp} values of 24.7 and $25.3\,K^{-1}\,mol^{-1}$ were observed. Therefore, it can be considered that ionic motions with a large degree of freedom exist in their solid phases.

The results of electric conductivity (σ) measurements are plotted in Figure 2. Because the $NEtPr_3BBu_4$ crystal indicated a low T_{mp} of 295.2 K, temperature dependences of σ values could not be obtained. In the case of $NEt_xMe_{(4-x)}BBu_4$ ($x = 1-3$) crystals, negative slopes were observed in the narrow temperature range. These changes can be attributed to effects of phase transition, because T_{tr1} and T_{tr2} were detected at these temperature ranges. A function of $\log(\sigma T)$ shows the activation energy (E_a) of ionic diffusion by the following relationship:

$$\log(\sigma T) \propto -\frac{E_a}{RT}. \quad (1)$$

Plotting $\log(\sigma T)$ as a function of T^{-1}, the slope gives the activation energies. The obtained E_a values are summarized in Table 1. The activation energies estimated in these compounds are similar to those reported in new-type ionic plastic crystals of BEt_3Me salts [30], although ΔS_{mp} values of $NEt_xMe_{(4-x)}BBu_4$ ($x = 1-3$) were unsatisfied to the condition of plastic crystal ($\Delta S_{mp} < 20\,J\,K^{-1}\,mol^{-1}$ [1]).

3.2. *NMR Results of $NEtMe_3BBu_4$, $NEt_2Me_2BBu_4$, and NEt_3MeBBu_4*

^1H and ^{13}C NMR spectra observed in $NEtMe_3BBu_4$, $NEt_2Me_2BBu_4$, and NEt_3MeBBu_4 crystals are displayed in Figure 3. In the case of $NEtMe_3BBu_4$, the ^1H MAS NMR lines recorded at 295 K showed broad peaks as displayed in Figure 3a. These peak intensities increased with temperature and new peaks were recorded in Phase II. Eight sharp signals were recorded on the ^1H MAS NMR spectrum at 350 K. This number is inconsistent with the chemical formula of $NEtMe_3BBu_4$, because spinning-side-band (SSB) signals would be recorded at 16.7 ppm intervals from an isotropic signal in the measurement condition of MAS = 10 kHz at 600.13 MHz. In addition, two broad lines were recorded at ca. 1.5 and 3.3 ppm in the whole temperatures. Based on these results, it can be concluded that $NEtMe_3BBu_4$ has a few sites in the crystal: Certain cations and anions have motions reducing $^1H-{}^1H$ dipole–dipole interactions and the others are restricted in the crystal. In the case of ^{13}C MAS NMR spectra, chemical-shift-anisotropy (CSA) line-shapes were recorded on the static spectrum at room temperature as shown in Figure 3b. This result is consistent with that of the ^1H MAS NMR spectrum at 295 K: Ionic motions are restricted at room temperature. The signals detected in a range from 50 to 70 ppm can be assigned to carbon atoms of $N(\underline{C}H_2CH_3)(\underline{C}H_3)_3^+$. The line-widths of 13.2 ppm are smaller than 21.9 and 85.0 ppm estimated by our CS simulation. Therefore, it can be considered that some of the cations perform overall motions at room temperature. This model can explain the ^1H MAS NMR spectra in which sharp lines were recorded.

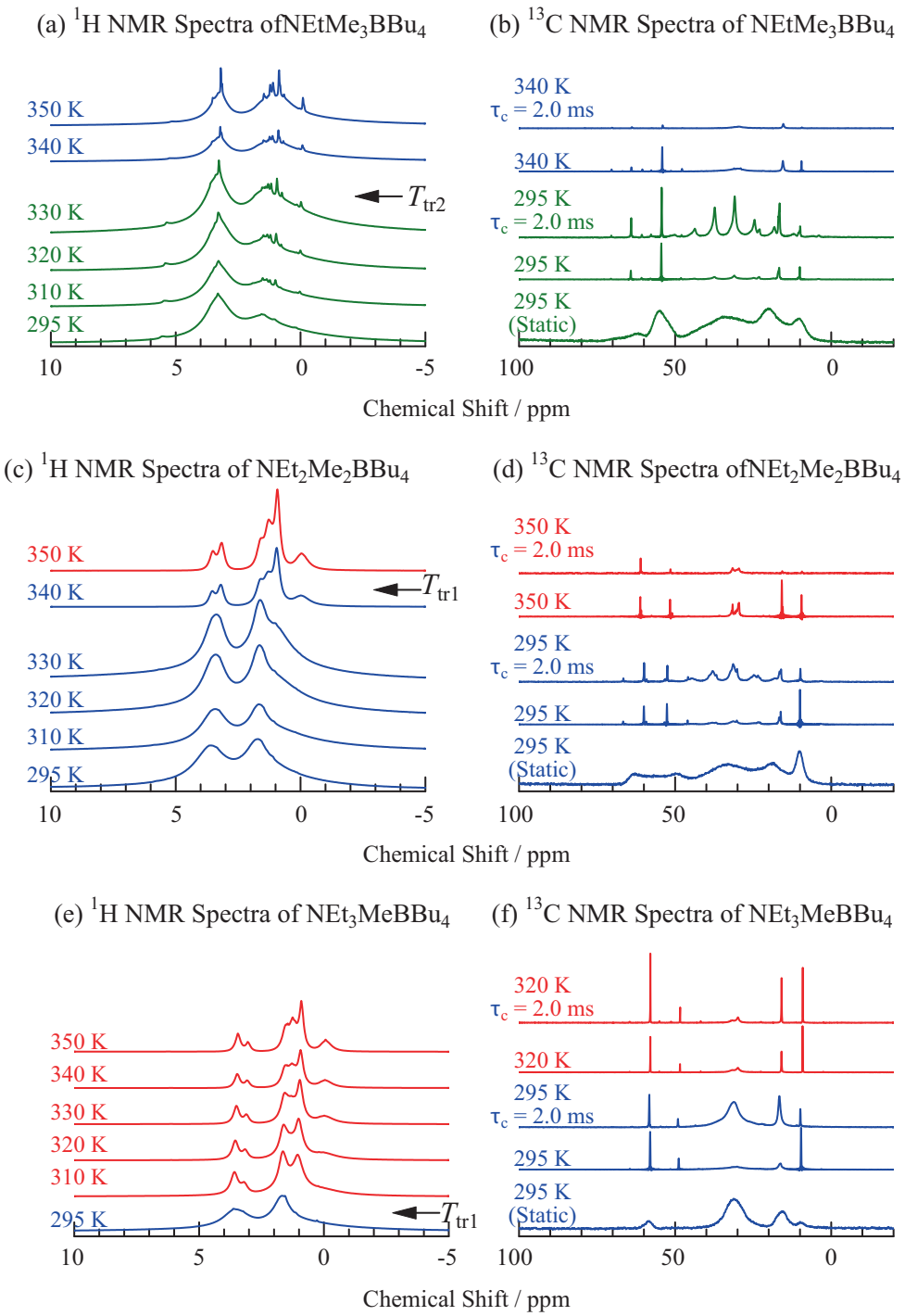

Fig. 3 (colour online). ^{1}H MAS and ^{13}C NMR spectra of NEtMe$_3$BBu$_4$, NEt$_2$Me$_2$BBu$_4$, and NEt$_3$MeBBu$_4$ as a function of temperature. In this figure, spectra recorded in Phase I, II, and III are shown by red, blue, and green lines, respectively. (a), (c), (e) ^{1}H MAS NMR lines were observed at a MAS ratio of 10 kHz. (b), (d), (f) ^{13}C MAS NMR spectra measurements were performed at MAS = 1 kHz. Contact times (τ_c) are described on ^{13}C CP/MAS NMR spectra.

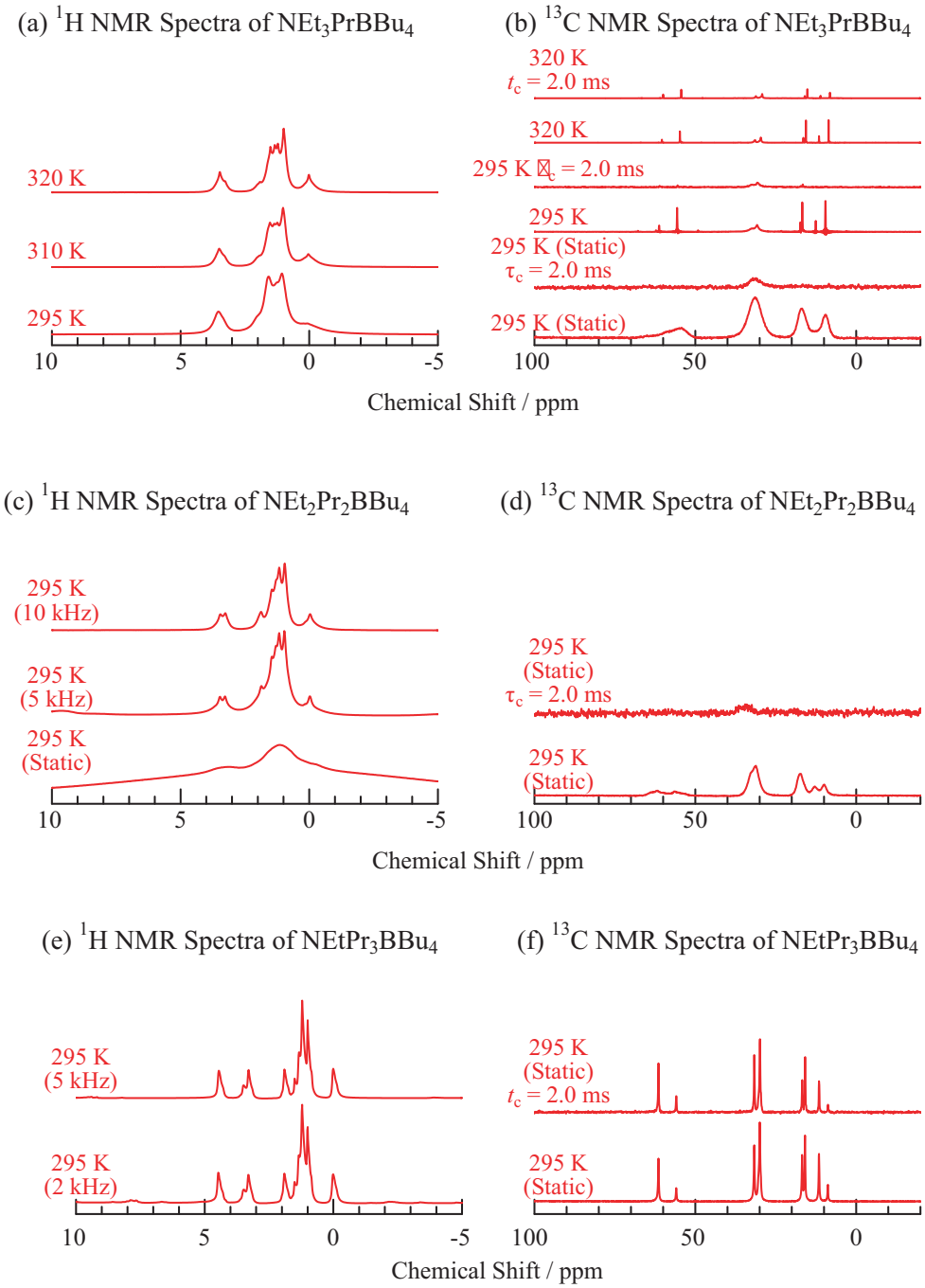

Fig. 4 (colour online). ^{1}H MAS and ^{13}C NMR spectra in Phase I of NEt_3PrBBu_4, $NEt_2Pr_2BBu_4$, and $NEtPr_3BBu_4$ crystals. (a) ^{1}H MAS NMR lines of NEt_3PrBBu_4 were observed at a MAS ratio of 10 kHz. (b) ^{13}C MAS NMR spectra measurements were performed at MAS = 1 kHz in NEt_3PrBBu_4. Contact times (τ_c) are described on ^{13}C CP/MAS NMR spectra. (c) ^{1}H MAS NMR lines of NEt_3PrBBu_4 were observed at some MAS ratios described in parenthesis. (d) Static ^{13}C CP NMR spectra measurements were performed at τ_c of 0 and 2.0 ms. (e) ^{1}H MAS NMR lines of $NEtPr_3BBu_4$ were observed at some MAS ratio described in parenthesis. (f) Static ^{13}C CP NMR spectra were observed at τ_c of 0 and 2.0 ms.

Conversely, the line-breadth observed at 39.8 ppm (this signal is assignable to the α-C atoms in the BBu_4^- ion) was similar to the calculated value of 37.22 ppm. Comparing the ^{13}C CP/MAS and MAS NMR spectra, the peak intensities of the anion were enhanced by the CP method, although the signals of the cation were independent. The later result also supports the tumbling motions of the cation, because overall motions modify the Hartmann–Hahn condition [34]. In the case of the anion's peak, the recorded line-width at 30.5 ppm became large after T_{tr2}. In general, the line-width of ^{13}C MAS NMR spectra is determined by CSA, dipole–dipole interaction, distribution, etc. As natural abundant samples and ^1H decoupling pulse sequence were employed in this study, it can be considered that there are some sites for anions in the crystal (CSA is generally reduced with increasing temperatures). This result is also consistent with the model in which the NEt_3MeBBu_4 crystal has some ion sites. Based on the NMR results and small ΔS_{tr1} of 8.7 $J\,K^{-1}\,mol^{-1}$, it can be considered that both the cation and anion have no isotropic reorientation in Phase I.

In the case of the $NEt_2Me_2BBu_4$ crystal, two broad signals were obtained on the ^1H MAS NMR spectra in Phase II as shown in Figure 3c. With increasing temperatures, new peaks were recorded at -0.02, 0.92, and 1.28 ppm in Phase I. These signals can be attributed to the hydrogen atoms of the BBu_4^- ion, therefore, it can be considered that the anions are restricted in Phase II and perform overall motions with large amplitudes in Phase I. Since the other signals detected at 1.58, 3.16, and 3.51 ppm in Phase I were attributable to the hydrogen atoms of $NCH_2C\underline{H}_3$, $NC\underline{H}_3$, and $NC\underline{H}_2CH_3$ in the $NEt_2Me_2^+$ ion, respectively, the cation also has overall motions with large amplitudes. The intensities of ^{13}C MAS NMR signals at 16.0, 30.1, and 31.4 ppm, which can be assigned to anion's peaks, were increased by applying the CP pulse sequence in Phase II as displayed in Figure 3d. These anion's peaks accompanied with SSB lines. In contrast, CP effects were not prevalent and small line-widths were recorded in Phase I. These results suggest that the anion performs overall motions with large amplitudes in Phase I. This conclusion is consistent with the ^1H MAS NMR spectra results. In the case of the cation's peak, the signal intensities were decreased by applying the CP pulse sequence, therefore, it can be considered that the cation also performs overall motions (tumbling) with large amplitudes in Phase I.

Similar tendencies were found on the ^1H and ^{13}C NMR spectra of the NEt_3MeBBu_4 crystal as displayed in Figure 3e and Figure 3f. The ^1H MAS NMR signals of NEt_3MeBBu_4 became narrow and intensities of the anion's peak at -0.06 ($BC\underline{H}_2C_3H_7$), 0.91 ($BC_3H_6C\underline{H}_3$), and 1.26 ppm ($BCH_2C_2\underline{H}_4CH_3$) increased with temperature. ^{13}C NMR line-intensities of the cation were independent of the CP method, although those of the anion were enhanced at 295 K. As SSB signals were observed in the ^{13}C MAS NMR spectra until 320 K, it can be concluded that there is no isotropic rotation in the crystal. Based on these results, it can be considered that the similar motions of the cation and anion are observed in $NEt_2Me_2BBu_4$ and NEt_3MeBBu_4.

3.3. NMR Results of NEt_3PrBBu_4, $NEt_2Pr_2BBu_4$, and $NEtPr_3BBu_4$

^1H and ^{13}C NMR spectra of the NEt_3PrBBu_4, $NEt_2Pr_2BBu_4$, and $NEtPr_3BBu_4$ crystals are displayed in Figure 4. In the case of NEt_3PrBBu_4, ^1H MAS NMR lines recorded in Phase I showed that the intensities of sharp components recorded at 0.01, 0.99, 1.22, 1.34, 1.51, 1.91, 3.25, and 3.47 ppm, which can be attributed to $BC\underline{H}_2C_3H_7$, $BC_3H_6C\underline{H}_3$, $BC_2H_4C\underline{H}_2CH_3$, $BCH_2C\underline{H}_2C_2H_5$, $NC_2H_4C\underline{H}_3$, $NCH_2C\underline{H}_3$, $NCH_2C\underline{H}_2CH_3$, $NC\underline{H}_2CH_3$, and $NC\underline{H}_2C_2H_5$, respectively, gradually increased with temperature as shown in Figure 4a. The static spectrum of ^{13}C nuclei showed narrow signals as shown in Figure 4b. These line-widths are clearly smaller than those of the other salts without $NEt_2Pr_2BBu_4$ and $NEtPr_3BBu_4$ treated in this study. Additionally, there were little CP effect on signal intensities and no SSB lines. Based on the NMR and DSC results, it can be concluded that both cation and anion perform isotropic reorientation in the crystal.

In the case of $NEt_2Pr_2BBu_4$, the melting point was observed at 307.9 K, therefore spinning ratio dependences of ^1H MAS NMR spectra were measured at room temperature. Independent spectra on MAS speeds were obtained as displayed in Figure 4c. This result suggests that the dipole–dipole interaction among the hydrogen atoms is reduced by ionic motions at ambient temperature. In addition, small line-breadth was recorded on the static ^1H NMR spectrum of the $NEt_2Pr_2BBu_4$ crystal. In ordinal compounds, dipole–dipole interactions among hydrogen atoms make line-

widths of a few tens of ppm on a static ^{1}H NMR spectrum. This fact also supports isotropic reorientation of both ions in the $NEt_2Pr_2BBu_4$ crystal. ^{13}C NMR spectra also indicate isotropic reorientation of the ions in the crystal, because only slight CP effects and narrow line-widths were recorded on the static spectra, as shown in Figure 4d.

In the case of $NEtPr_3BBu_4$, a low melting point of 295.2 K was obtained by DSC measurement. Because of the low T_{mp}, we could obtain ^{1}H and ^{13}C NMR spectra in partially fused samples, as shown in Figures 4e and 4f.

3.4. Comparing With BEt_3Me Salts

Two cations of NEt_3Pr^+ and $NEt_2Pr_2^+$ showed isotropic reorientation motions and low ΔS_{mp} with BBu_4^- anions, although whole cations of $NEtMe_3^+$, $NEt_2Me_2^+$, NEt_3Me^+, NEt_3Pr^+, $NEt_2Pr_2^+$, and $NEtPr_3^+$ can form plastic crystals with BEt_3Me^- [30]. This difference can be explained by the anion's volume. The B3LYP/6-311+G** simulation showed an ion radius (distance from the boron atom to the terminal carbon atom) of 268 and 534 pm for BEt_3Me^- and BBu_4^- ions, respectively. In the case of the former, the majority of space in the anion is shared by the hydrogen and carbon atoms of itself, therefore, cations cannot insert into the anion's space. Conversely, the vacant of the BBu_4^- ion is larger than that of the BEt_3Me^- ion. Therefore, the model in which a part of the small cation, e. g. NMe_3Et^+, penetrates into the BBu_4^- ion can be constructed. Since the BEt_3Me^- ion can eliminate penetration, it can be regarded that BEt_3Me^- ions can form ionic plastic crystals with many cations in an analogous size. In the case of the BBu_4 salts, tumbling motions of cations could be detected in $NEtMe_3BBu_4$, $NEt_2Me_2BBu_4$, and NEt_3MeBBu_4, and isotropic reorientation was observed in NEt_3PrBBu_4 and $NEt_2Pr_2BBu_4$. In the case of σ measurements, similar E_a values for ionic translation motion were recorded in new ionic plastic crystals (NEt_3PrBBu_4 and $NEt_2Pr_2BBu_4$) and non-plastic crystals ($NEtMe_3BBu_4$, $NEt_2Me_2BBu_4$, and $NEtMe_3BBu_4$). Based on these results, it can be regarded that overall motions with large amplitudes (tumbling) can perform the resemble effect as isotropic reorientation, i. e. preventing insertion of the counter ions into themselves.

4. Conclusion

This study reveals that two compounds of NEt_3PrBBu_4 and $NEt_2Pr_2BBu_4$ are new ionic plastic crystals. Based on our results of ^{1}H and ^{13}C NMR spectra, DSC, and electric conductivity measurements, both globular cations and anions undergo isotropic reorientation and self-diffusion. NMR measurements also reveal that $NEtMe_3BBu_4$, $NEt_2Me_2BBu_4$, and NEt_3MeBBu_4 have a tumbling motion in each crystal. In addition, σ measurements showed low activation energies for self-diffusion in these crystals. This result suggests that the mechanism of ion transfer is analogous to molecular plastic crystal rather than ordinal ionic plastic crystal assembled by a globular ion and a non-globular counter ion. In the case of BEt_3Me salts, isotropic reorientation is reported in $NEt_xR'_{(4-x)}BEt_3Me$ ($x = 1-3$, R′ = Me, Pr) [30]. In contrast, it was detected in two BBu_4 compounds of NEt_3PrBBu_4 and $NEt_2Pr_2BBu_4$ (NR_4BBu_4 (R = Me, Et, Pr, Bu, Pen) has no plastic-crystal phases [31]). This difference between BBu_4 and BEt_3Me can be considered as a collision between the long alkyl chains of anion and cation.

Acknowledgements

The authors are grateful to Prof. H. Tsukada of Yokohama City University for useful instruction of organic synthesis and to Prof. H. Fujimori of Nihon University for the use of the SSC/5200 calorimeter. This work was partly supported by a Grant-in-Aid for Scientific Research (23550230) from the Japan Society for the Promotion of Science.

[1] J. Timmermans, J. Phys. Chem. Solids. **18**, 1 (1961).
[2] Yu. M. Solonin, V. F. Gorban, and E. A. Graivoronskaya, Dopovidi Natsional'noi Akademii Nauk Ukraini **4**, 114 (2008).
[3] W. I. F. David, Appl. Rad. Iso. **46**, 519 (1995).
[4] Y. Jin, A. Xenopoulos, J. Cheng, W. Chen, B. Wunderlich, M. Diack, C. Jin, R. L. Hettich, R. N. Compton, and G. Guiochon, Mol. Cryst. Liq. Cryst. Sci. Techn. A **257**, 235 (1994).
[5] S. Takeda and T. Atake, Kotai Butsuri **28**, 183 (1993).
[6] G. Burns, F. H. Dacol, and B. Welber, Solid State Commun. **32**, 151 (1979).
[7] M. Debeau and P. Depondt, J. Chimie Physique Phys.-Chimie Bio. **82**, 233 (1985).

[8] S. Ganguly, J. R. Fernandes, and C. N. R. Rao, Adv. Molec. Relax. Interact. Proc. **20**, 149 (1981).
[9] K. Kobashi and R. D. Etters, Molecular Phys. **46**, 1077 (1982).
[10] K. Moriya, T. Matsuo, and H. Suga, Thermochim. Acta **132**, 133 (1988).
[11] K. Moriya, T. Matsuo, and H. Suga, Bull. Chem. Soc. Jpn. **61**, 1911 (1988).
[12] K. Moriya, T. Matsuo, and H. Suga, Chem. Phys. Lett. **82**, 581 (1981).
[13] K. Moriya, T. Matsuo, and H. Suga, Chem. Lett. **1977**, 1427 (1977).
[14] K. Moriya, T. Matsuo, and H. Suga, J. Phys. Chem. Solids **44**, 1103 (1983).
[15] Y. Furukawa and H. Kiriyama, Chem. Phys. Lett. **93**, 617 (1982).
[16] Y. Furukawa, H. Nagase, R. Ikeda, and D. Nakamura, Bull. Chem. Soc. Jpn. **64**, 3105 (1991).
[17] M. Kenmotsu, H. Honda, H. Ohki, R. Ikeda, T. Erata, A. Tasaki, and Y. Furukawa, Z. Naturforsch. **49a**, 247 (1994).
[18] H. Honda, M. Kenmotsu, H. Ohki, R. Ikeda, and Y. Furukawa, Ber. Bunsenges. Phys. Chem. **99**, 1009 (1995).
[19] H. Honda, S. Ishimaru, N. Onoda-Yamamuro, and R. Ikeda, Z. Naturforsch. **50a**, 871 (1995).
[20] H. Honda, M. Kenmotsu, N. Onoda-Yamamuro, H. Ohki, S. Ishimaru, R. Ikeda, and Y. Furukawa, Z. Naturforsch. **51a**, 761 (1996).
[21] H. Honda, N. Onoda-Yamamuro, S. Ishimaru, R. Ikeda, O. Yamamuro, and T. Matsuo, Ber. Bunsenges. Phys. Chem. **102**, 148 (1998).
[22] N. Onoda-Yamamuro, H. Honda, R. Ikeda, O. Yamamuro, T. Matsuo, K. Oikawa, and F. Izumi, J. Phys. Condens. Matter **10**, 3341 (1998).
[23] H. Honda, Z. Naturforsch. **62a**, 633 (2007).
[24] R. Ikeda, Recent Res. Devel. Chem. Physics **5**, 257 (2004).
[25] J. Adebahr, M. Grimsley, N. M. Rocher, D. R. MacFarlane, and M. Forsyth, Solid State Ionics **178**, 1793 (2008).
[26] A. J. Seeber, M. Forsyth, C. M. Forsyth, S. A. Forsyth, G. Annat, and D. R. MacFarlane, Phys. Chem. Chem. Phys. **5**, 2692 (2003).
[27] H. Ono, S. Ishimaru, and R. Ikeda, Ber. Bunsenges. Phys. Chem. **102**, 650 (1998).
[28] H. Ono, S. Ishimaru, R. Ikeda, and H. Ishida, Bull. Chem. Soc. Jpn. **72**, 2049 (1999).
[29] H. Honda, S. Ishimaru, and R. Ikeda, Z. Naturforsch. **54a**, 519 (1999).
[30] T. Hayasaki, S. Hirakawa, and H. Honda, Bull. Chem. Soc. Jpn. **86**, 993 (2013).
[31] T. Hayasaki, S. Hirakawa, and H. Honda, Am. Chem. Sci. J. (2014) in press.
[32] J. Kabatc and J. Paczkowski, Dyes Pigm. **61**, 1 (2004).
[33] M. J. Frisch, G. W. Trucks, H. B. Schlegel, G. E. Scuseria, M. A. Robb, J. R. Cheeseman, J. A. Montgomery, T. Vreven, K. N. Kudin, J. C. Burant, J. M. Millam, S. S. Iyengar, J. Tomasi, V. Barone, B. Mennucci, M. Cossi, G. Scalmani, N. Rega, G. A. Petersson, H. Nakatsuji, M. Hada, M. Ehara, K. Toyota, R. Fukuda, J. Hasegawa, M. Ishida, T. Nakajima, Y. Honda, O. Kitao, H. Nakai, M. Klene, X. Li, J. E. Knox, H. P. Hratchian, J. B. Cross, C. Adamo, J. Jaramillo, R. Gomperts, R. E. Stratmann, O. Yazyev, A. J. Austin, R. Cammi, C. Pomelli, J. W. Ochterski, P. Y. Ayala, K. Morokuma, G. A. Voth, P. Salvador, J. J. Dannenberg, V. G. Zakrzewski, S. Dapprich, A. D. Daniels, M. C. Strain, O. Farkas, D. K. Malick, A. D. Rabuck, K. Raghavachari, J. B. Foresman, J. V. Ortiz, Q. Cui, A. G. Baboul, S. Clifford, J. Cioslowski, B. B. Stefanov, G. Liu, A. Liashenko, P. Piskorz, I. Komaromi, R. L. Martin, D. J. Fox, T. Keith, M. A. Al-Laham, C. Y. Peng, A. Nanayakkara, M. Challacombe, P. M. W. Gill, B. Johnson, W. Chen, M. W. Wong, C. Gonzalez, and J. A. Pople, Gaussian 03, Revision B.04, Gaussian, Inc., Pittsburgh PA, 2003.
[34] H. Saito, S. Tuzi, M. Tanio, and A. Naito, Annu. Rep. NMR Spectr. **47**, 39 (2001).